Modeling all exceedances above a threshold using an extremal dependence structure: Inferences on several flood characteristics

M. Ribatet,[1] T. B. M. J. Ouarda,[2] E. Sauquet,[3] and J.-M. Gresillon[3]

Received 5 July 2007; revised 24 November 2008; accepted 12 January 2009; published 10 March 2009.

[1] Flood quantile estimation is of great importance for several types of engineering studies and policy decisions. However, practitioners must often deal with the limited availability of data and with short-length observation series. Thus, the information must be used optimally. During the last decades, to make better use of available data, inferential methodology has evolved from annual maxima modeling to peaks over a threshold. To mitigate the lack of data, peaks over a threshold are sometimes combined with additional information, mostly regional or historical information. However, the most important information for the practitioner remains the data available at the target site. In this study, a model that allows inference on the whole time series is introduced. In particular, the proposed model takes into account the dependence between successive extreme observations using an appropriate extremal dependence structure. Results show that this model leads to more accurate flood peak quantile estimates than conventional estimators. In addition, as the time dependence is taken into account, inferences on other flood characteristics can be performed. An illustration is given with flood duration data. Our analysis shows that the accuracy of the proposed models to estimate flood duration is related to specific catchment characteristics. Some suggestions to increase the flood duration predictions are presented.

Citation: Ribatet, M., T. B. M. J. Ouarda, E. Sauquet, and J.-M. Gresillon (2009), Modeling all exceedances above a threshold using an extremal dependence structure: Inferences on several flood characteristics, *Water Resour. Res.*, *45*, W03407, doi:10.1029/2007WR006322.

1. Introduction

[2] Estimation of extreme flood events is important for several engineering design and risk management activities. This is a considerable task as the amount of data available is often limited. Thus, to increase the precision and the quality of the estimates, several authors resorted to the use of other sources of information. For example, *Chebana and Ouarda* [2008], *Ribatet et al.* [2007a], *Kjeldsen and Jones* [2006, 2007], and *Cunderlik and Ouarda* [2006] used information from other homogeneous gauging stations. *Werritty et al.* [2006] and *Reis and Stedinger* [2005] used historical information to improve inferences. Incorporation of additional information in the estimation procedure is attractive but it should not be more prominent than the original target site data [*Ribatet et al.*, 2007b]. Before looking for other sources of information, it seems reasonable to use efficiently the data available at the target site. Most often, practitioners possess initially the whole time series rather than only the extreme observations. In particular, the reduction of a time series to a sample of annual maxima (AM) represents a loss of information.

[3] In this perspective, the peaks over threshold (POT) [*Ashkar and Rousselle*, 1987; *Madsen and Rosbjerg*, 1997] approach is less wasteful as more than one event per year can be inferred. However, the declustering method used to identify independent events is quite subjective. Furthermore, even though a ''quasi automatic'' procedure was recently introduced by *Ferro and Segers* [2003], there is still a waste of information as only cluster maxima are used.

[4] *Coles et al.* [1994] and *Smith et al.* [1997] proposed an approach based on Markov chain models that uses all exceedances and accounts for temporal dependence between successive observations. Finally, the entire information available within the time series is taken into account. More recently, *Fawcett and Walshaw* [2006] gave an illustrative application of the Markov chain model to extreme wind speed modeling.

[5] In the present study, extreme flood events are of interest. The performance of the Markov chain model is compared to the conventional POT approach. The data analyzed consist of a collection of 50 French gauging stations. These stations constituted a subset of the data set formed by *Renard et al.* [2008] to examine stationarity of hydrological extremes in France. The area under study ranges from 2°W to 7°E and from 45°N to 51°N. The drainage areas vary from 72 to 38300 km^2 with a median value of 792 km^2. Daily observations were recorded from 39 to 105 years, with a mean value of 60 years. For the remainder of this article, the quantile benchmark values are

[1]Institute of Mathematics, Ecole Polytechnique Federale de Lausanne, Lausanne, Switzerland.
[2]INRS-ETE, University of Quebec, Quebec, Quebec, Canada.
[3]Cemagref Lyon, Unite de Recherche Hydrologie-Hydraulique, Lyon, France.

0043-1397/09/2007WR006322$09.00

derived from the maximum likelihood estimates on the whole times series using a conventional POT analysis.

[6] The paper is organized as follows: section 2 introduces the theoretical aspects for the Markov chain model, while section 3 checks the relevance of the Markovian model hypothesis. Sections 4 and 5 analyze the performance of the Markovian model to estimate the flood peaks and durations respectively. Finally, some conclusions and perspectives are presented in section 6.

2. Markov Chain Model for Cluster Exceedances

[7] In this section, the extremal Markov chain model is presented. In the remainder of this article, it is assumed that the flow Y_t at time t depends on the value Y_{t-1} at time $t-1$. In this flexible formulation, Y_t represents the streamflow at any time scale t. In hydrology, the daily time scale is often used. In this case Y_t represents the daily streamflow for day t. However, the model remains valid for any time scale, e.g., hourly scale. The dependence between two consecutive observations is modeled by a first-order Markov chain. Before introducing the theoretical aspects of the model, it is worth justifying and describing the main advantages of the proposed approach.

[8] It is now well known that the univariate extreme value theory (EVT) is relevant when modeling either AM or POT data series. Nevertheless, its extension to the multivariate case is surprisingly rarely applied in practice. Recently the use of the multivariate framework to treat hydrological extreme events has been receiving additional attention. Several applications made use of bivariate distributions and copulas to jointly model the various components of extreme hydrological events, for instance flood peak, volume and duration [*Yue et al.*, 2001; *Zhang and Singh*, 2006], drought magnitude, volume and duration [*Ashkar et al.*, 1998; *Ouarda et al.*, 2008], and storm intensity and duration [*Salvadori and De Michele*, 2004]. The adoption of the multivariate framework to treat extreme hydrological events was motivated by the fact that single-variable hydrological analysis provides limited understanding and assessment of the true behavior of hydrological phenomena which are often characterized by a set of correlated random variables. Recent research is starting to focus on the development of regional multivariate modeling tools [*Chebana and Ouarda*, 2007]. A common element in all research dealing with the use of multivariate tools for the analysis of extreme hydrological events is the attempt to maximize the use of all available hydrological information to improve inference concerning rare events.

[9] The present work aims to motivate the use of the multivariate EVT (MEVT). In our application, the multivariate results are used to model the dependence between a set of lagged values in a times series. Consequently, compared to the AM or the POT approaches, the amount of observations used in the inference procedure is clearly larger. For instance, while only cluster maxima are used in a POT analysis, all exceedances are inferred using a Markovian model. In this sense, the proposed approach lies between POT analysis and conventional time series analysis. Indeed, time series analysis is interested in the dependence structure for the whole time series including low streamflow values, while the proposed approach focuses on the dependence structure between successive extreme observations. POT modeling, on the other hand, leads to the loss of a significant part of extreme values as only (independent) flood peaks are considered.

2.1. Likelihood Function

[10] Let $Y_1, \ldots, Y_n$ be a stationary first-order Markov chain with a joint distribution function of two consecutive observations $F(y_1, y_2)$, and $F(y)$ its marginal distribution. Thus, the likelihood function L evaluated at the n first daily streamflow values $(y_1, \ldots, y_n)$ is

$$L(y_1, \ldots, y_n) = f(y_1) \prod_{i=2}^{n} f(y_i|y_{i-1}) = \frac{\prod_{i=2}^{n} f(y_i, y_{i-1})}{\prod_{i=2}^{n-1} f(y_i)} \quad (1)$$

where $f(y_i)$ is the marginal density, $f(y_i|y_{i-1})$ is the conditional density, and $f(y_i, y_{i-1})$ is the joint density of the $i-1$ and i daily observations.

[11] To model all exceedances above a sufficiently large threshold u, the joint and marginal densities must be known. Standard univariate EVT arguments [*Coles*, 2001] justify the use of a generalized Pareto distribution (GPD) for $f(y_i)$, e.g., a term of the denominator in equation (1). As a consequence, the marginal distribution is defined by

$$F(y) = 1 - \lambda\left(1 + \xi\frac{y-u}{\sigma}\right)^{-1/\xi}, \qquad y \geq u \quad (2)$$

where $1 + \xi(y-u)/\sigma > 0$, $\lambda = \Pr[Y \geq u]$, σ and ξ are respectively the scale and shape parameters. Similarly, MEVT arguments [*Resnick*, 1987] justify the use of a bivariate extreme value distribution for $f(y_i, y_{i-1})$, e.g., a term of the numerator in equation (1). Thus, the joint distribution is defined by

$$F(y_1, y_2) = \exp[-V(z_1, z_2)], \qquad y_1 \geq u, \quad y_2 \geq u \quad (3)$$

where V is a homogeneous function of order -1, e.g., $V(nz_1, nz_2) = n^{-1}V(z_1, z_2)$, satisfying $V(z_1, \infty) = z_1^{-1}$ and $V(\infty, z_2) = z_2^{-1}$, and $z_i = -1/\log F(y_i)$, $i = 1, 2$.

[12] Unlike the univariate case, there is no finite parametrization for the V functions. Thus, it is common to use specific parametric families for V such as the logistic [*Gumbel*, 1960], the asymmetric logistic [*Tawn*, 1988], the negative logistic [*Galambos*, 1975], or the asymmetric negative logistic [*Joe*, 1990] models. Some details for these parametrizations are reported in Appendix A. These models, as all models of the form (3) are asymptotically dependent, that is [*Coles et al.*, 1999],

$$\chi = \lim_{\omega \to 1} \chi(\omega) = \lim_{\omega \to 1} \Pr[F(Y_2) > \omega | F(Y_1) > \omega] > 0 \quad (4)$$

$$\overline{\chi} = \lim_{\omega \to 1} \overline{\chi}(\omega) = \lim_{\omega \to 1} \frac{2\log(1-\omega)}{\log \Pr[F(Y_1) > \omega, F(Y_2) > \omega]} - 1 = 1 \quad (5)$$

[13] Other parametric families exist to consider simultaneously asymptotically dependent and independent cases [*Bortot and Tawn*, 1998]. However, apart from a few particular cases (see section 3), the data analyzed here

seems to belong to the asymptotically dependent class. Consequently, in this work, only asymptotically dependent models are considered, i.e., of the form (1)–(3).

2.2. Inference

[14] The Markov chain model is fitted using maximum censored likelihood estimation [*Ledford and Tawn*, 1996]. The contribution $L_n(y_1, y_2)$ of a two consecutive daily streamflow values y_1, y_2 to the numerator of equation (1) is given by

$$L_n(y_1,y_2) = \begin{cases} \exp[-V(z_1,z_2)][V_1(z_1,z_2)V_2(z_1,z_2) - V_{12}(z_1,z_2)]K_1K_2, & \text{if } y_1 > u, y_2 > u \\ \exp[-V(z_1,z_2)]V_1(z_1,z_2)K_1, & \text{if } y_1 > u, y_2 \le u \\ \exp[-V(z_1,z_2)]V_2(z_1,z_2)K_2, & \text{if } y_1 \le u, y_2 > u \\ \exp[-V(z_1,z_2)], & \text{if } y_1 \le u, y_2 \le u \end{cases} \quad (6)$$

where $K_j = -\lambda_j\sigma^{-1}t_j^{1+\xi}z_j^2\exp(1/z_j)$, $t_j = [1 + \xi(y_j - u)/\sigma]_+^{-1/\xi}$ and V_j, V_{12} are respectively the partial derivative with respect to the component j and the mixed partial derivative. The contribution $L_d(y_j)$ of a daily streamflow y_j to the denominator of equation (1) is given by

$$L_d(y_j) = \begin{cases} \sigma^{-1}\lambda\left[1 + \xi(y_j - u)/\sigma\right]_+^{-1/\xi-1}, & \text{if } y_j > u, \\ 1 - \lambda, & \text{otherwise} \end{cases} \quad (7)$$

Finally, the log likelihood is given by

$$\log L(y_1,\ldots,y_n) = \sum_{i=2}^{n}\log L_n(y_{i-1},y_i) - \sum_{i=2}^{n-1}\log L_d(y_i) \quad (8)$$

2.3. Return Levels

[15] Most often, the main objective of an extreme value analysis is quantile estimation. As for the POT approach, return level estimates can be computed. However, as all exceedances are inferred, this is done in a different way as the dependence between successive observations must be taken into account. For a stationary sequence $Y_1, Y_2, \ldots, Y_n$ with a marginal distribution function F, *Lindgren and Rootzen* [1987] have shown that

$$\Pr[\max\{Y_1, Y_2, \ldots, Y_n\} \le y] \approx F(y)^{n\theta} \quad (9)$$

where $\theta \in [0, 1]$ is the extremal index and can be interpreted as the reciprocal of the mean cluster size [*Leadbetter*, 1983]; that is, $\theta = 0.5$ means that extreme (enough) events are expected to occur by pair. $\theta = 1$ ($\theta \to 0$) corresponds to the independent (perfect dependent) case.

[16] As a consequence, the quantile Q_T corresponding to the T-year return period is obtained by equating equation (9) to $1 - 1/T$ and solving for T. By definition, Q_T is the observation that is expected to be exceeded once every T years, i.e.,

$$Q_T = u - \sigma\xi^{-1}\left(1 - \left\{\lambda^{-1}\left[1 - (1 - 1/T)^{1/(n\theta)}\right]\right\}^{-\xi}\right) \quad (10)$$

It is worth emphasizing equation (9) as it has a large impact on both theoretical and practical aspects. Indeed, for the AM approach, equation (9) is replaced by

$$\Pr[\max\{Y_1, Y_2, \ldots, Y_n\} \le y] \approx G(y) \quad (11)$$

where G is the distribution function of the random variable $M_n = \max\{Y_1, Y_2, \ldots, Y_n\}$, that is a generalized extreme value distribution. In particular, equations (9) and (11) differ as the first one is fitted to the whole set of observations Y_i, while the latter is fitted to the AM ones. By definition, the number n_Y of the Y_i observations is much larger than the size n_M of the AM data set. Especially, for daily data, $n_Y = 365\ n_M$.

[17] From equation (10), the extremal index θ must be known to obtain quantile estimates. The methodology applied in this study is similar to the one suggested by *Fawcett and Walshaw* [2006]. Once the Markovian model is fitted, 100 Markov chains of length 2000 were generated. For each chain, the extremal index is estimated using the estimator proposed by *Ferro and Segers* [2003] to avoid issues related to the choice of declustering parameter. In particular, the extremal index θ is estimated using the following equations:

$$\hat{\theta}(u) = \begin{cases} \max\left(1, \dfrac{2\left[\sum_{i=1}^{N-1}(T_i - 1)\right]^2}{(N-1)\sum_{i=1}^{N-1}T_i^2}\right), & \text{if } \max\{T_i : 1 \le i \le N-1\} \le 2 \\ \max\left(1, \dfrac{2\left(\sum_{i=1}^{N-1}T_i\right)^2}{(N-1)\sum_{i=1}^{N-1}(T_i - 1)(T_i - 2)}\right), & \text{otherwise} \end{cases} \quad (12)$$

where N is the number of observations exceeding the threshold u, T_i is the interexceedance time, e.g., $T_i = S_{i+1} - S_i$ and S_i is the ith exceedance time.

[18] Lastly, the extremal index related to a fitted Markov chain model is estimated using the sample mean of the 100 extremal index estimations. Figure 1 represents the histogram of these 100 extremal index estimations. In this study, as a large number of time series is involved, the number and length of the simulated Markov chains may be too small to lead to the most accurate extremal index estimations; but

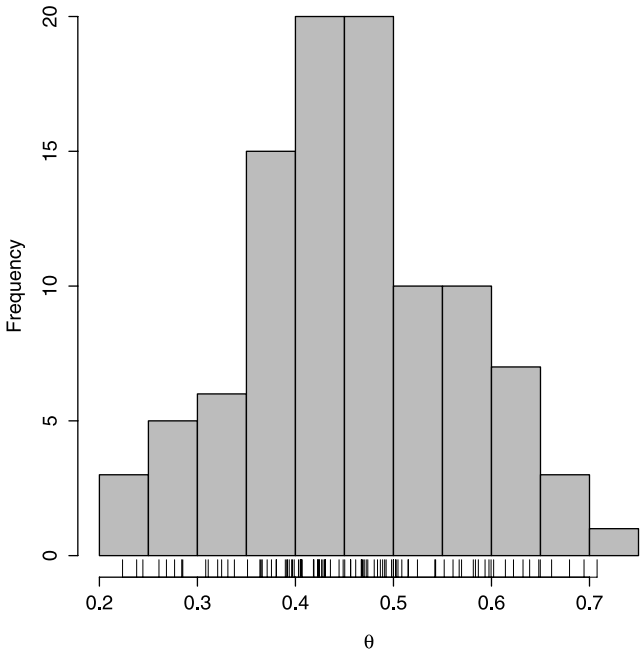

Figure 1. Histogram of the extremal index estimations from the 100 simulated Markov chains of length 2000.

avoid intractable CPU times. If less sites are considered, it is preferable to increase these two values.

[19] A preliminary study (not presented here) has shown that, for quantile estimation, this procedure was more accurate than estimating θ using the estimator of *Leadbetter* [1983]. This confirms the conclusions drawn by *Fawcett* [2005] for extreme wind speed data.

3. Extreme Value Dependence Structure Assessment

[20] Prior to performing any estimations, it is necessary to test whether: (1) the first-order Markov chain assumption and (2) the extreme value dependence structure (equation (3)) are appropriate to model successive observations above the threshold u. Figures 2 and 3 illustrate the autocorrelation functions and the scatterplots between two consecutive observations for two different gauging stations. As the partial autocorrelation coefficient at lag 1 is large, Figures 2 and 3 (left plots) corroborate the first hypothesis. However, some partial autocorrelation coefficients are significant beyond lag 1. This may suggest that a higher-order model may be more appropriate but does not necessarily mean that a first-order assumption is completely flawed. Simplex plots [*Coles and Tawn*, 1991] can be used to assess the suitability of a second-order assumption over a first-order one. For instance, if the points of the simplex plot are grouped in a cluster of points on the interior, this suggests that a second-order Markov chain might be more appropriate, though this doesn't necessarily imply that the first-order assumption will completely fail. On the other hand, if the points tend to lie toward the edge of the plot, pairwise dependence is implied. For our application, it seems that a first-order model seems to be valid, except for the three slowest dynamic catchments. Figure 4 consists of simplex plots for the stations K0523010, K4470010 and E6470910. These three simplex plots lead to three different conclusions: (1) the left plot advocates the use of the first-order assumption, (2) the middle plot suggests that a second-order Markov chain might be more appropriate and (3) the right plot clearly promotes the use of a second-order assumption. The middle plot corresponds to the three slowest dynamic catchments as stated above while the right plot is specific as station E6470910 has a major runoff contribution coming from groundwater flow.

[21] Though it is an important stage because of its consequences on quantile estimates [*Ledford and Tawn*, 1996; *Bortot and Coles*, 2000], verifying the second hypothesis is a considerable task. An overwhelming dependence between consecutive observations at finite levels is not sufficient as it does not give any information about the dependence relationship at asymptotic levels. For instance, the overwhelming dependence at lag 1 (Figures 2 and 3,

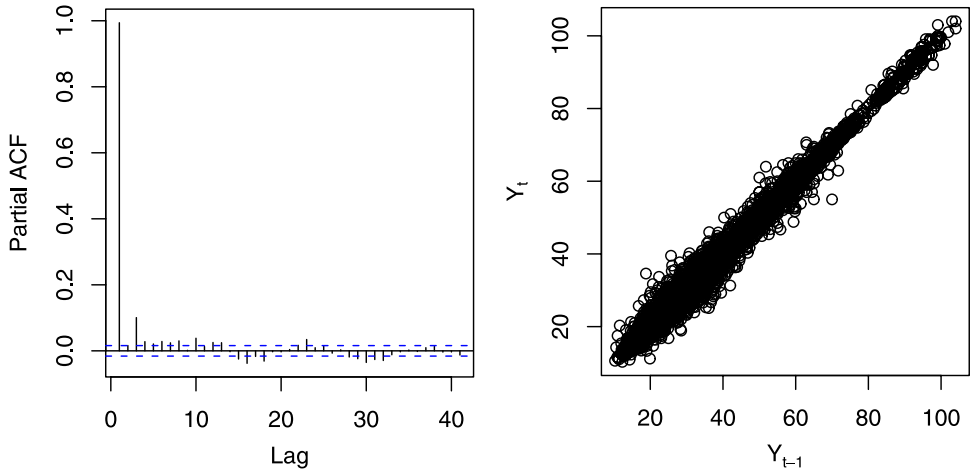

Figure 2. (left) Autocorrelation plot and (right) scatterplot of the time series at lag 1 for station E6470910.

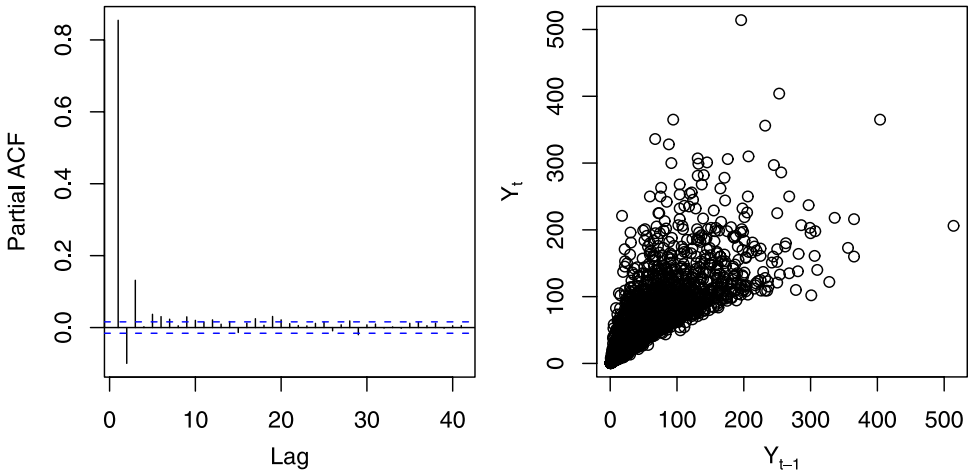

Figure 3. (left) Autocorrelation plot and (right) scatterplot of the time series at lag 1 for station A4200630.

right plots) does certainly not justify the use of an asymptotic dependent model.

[22] Figures 5 and 6 present the evolution of the $\chi(\omega)$ and $\overline{\chi}(\omega)$ statistics as ω increases for two different sites. For Figures 5 and 6, the confidence intervals are derived by bootstrapping contiguous blocks to take into account the successive observations dependence [*Ledford and Tawn*, 2003]. The $\chi(\omega)$ and $\overline{\chi}(\omega)$ statistics seem to depict two different asymptotic extremal dependence structures. From Figure 5, it seems that $\lim \chi(\omega) \gg 0$ and $\lim \overline{\chi}(\omega) = 1$ for $\omega \to 1$. On the contrary, Figure 6 advocates that $\lim \chi(\omega) = 0$ and $\lim \overline{\chi}(\omega) < 1$ for $\omega \to 1$. Consequently, Figure 5 seems to conclude for an asymptotically dependent case while Figure 6 for an asymptotically independent case.

[23] In theory, asymptotic (in)dependence should not be assessed using scatterplots. However, these two different features can be deduced from Figures 2 and 3. For Figure 2, the scatterplot (Y_{t-1}, Y_t) is increasingly less spread as the observations become larger; while increasingly more spread for Figure 3. In other words, for the first case, the dependence seems to become stronger at larger levels while it is the opposite for the second case.

[24] Two specific cases for different asymptotic dependence structures were illustrated. Table 1 shows the evolution of the $\chi(\omega)$ statistics as ω increases for all the sites under study. Most of the stations have significantly positive $\chi(\omega)$ values. In addition, only 13 sites have a 95% confidence interval that contains the 0 value. For 9 of these stations, the 95% confidence intervals correspond to the theoretical lower and upper bounds; so that uncertainties are too large to determine the extremal dependence class. For the $\overline{\chi}$ statistic, results are less clear cut. Figure 7 represents the histograms for $\overline{\chi}(\omega)$ for successive ω values. Despite only a few observations being close to 1, most of the stations have a $\overline{\chi}(\omega)$ value greater than 0.75. These values can be considered as significantly high as $-1 < \overline{\chi}(\omega) \leq 1$, for all ω. Consequently, models of the form (1)–(3) may be suited to model the extremal dependence between successive observations.

[25] Other methods exist to test the extremal dependence but were unconvincing for our application [*Ledford and Tawn*, 2003; *Falk and Michel*, 2006]. Indeed, the approach of *Falk and Michel* [2006] does not take into account the dependence between Y_{t-1} and Y_t; while the test of *Ledford*

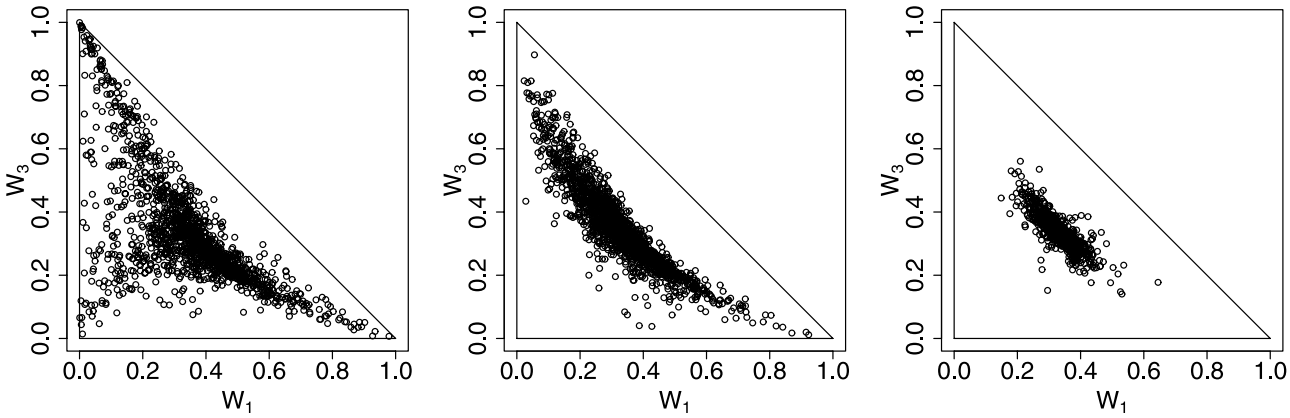

Figure 4. Simplex plots for stations (left) K0523010, (middle) K4470010, and (right) E6470910.

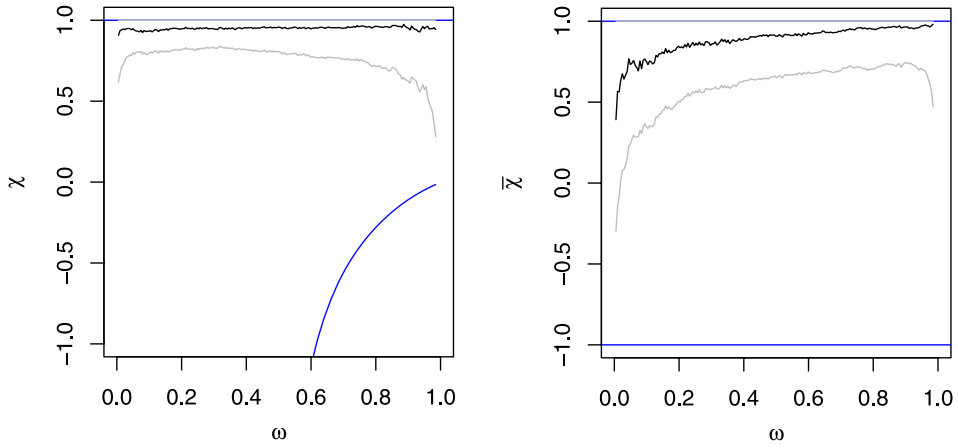

Figure 5. Plot of the χ and $\overline{\chi}$ statistics and the related 95% confidence intervals for station E6470910. The solid blue lines are the theoretical bounds.

and Tawn [2003] appears to be poorly discriminatory for our case study.

4. Performance of the Markovian Models on Quantile Estimation

4.1. Comparison Between Markovian Estimators

[26] In this section, the performance of six different extremal dependence structures is analyzed on the 50 gauging stations introduced in section 1. These models are: *log* for the logistic, *nlog* for the negative logistic, *mix* for the mixed models and their relative asymmetric counterparts, e.g., *alog*, *anlog* and *amix*. To assess the impact of the dependence structure on flood peak estimation, the efficiency of each model to estimate quantiles with return periods 2, 10, 20, 50 and 100 years is evaluated.

[27] As practitioners often have to deal with small record lengths in practice, the performance of the Markovian models is analyzed on all sub time series of length 5, 10, 15 and 20 years. Finally, to assess the efficiency for all the gauging stations considered in this study, the normalized bias (*nbias*), the variance (*var*) and the normalized mean squared error (*nmse*) are computed:

$$nbias = \frac{1}{N}\sum_{i=1}^{N}\frac{\hat{Q}_{i,T} - Q_T}{Q_T} \tag{13}$$

$$var = \frac{1}{N-1}\sum_{i=1}^{N}\left(\frac{\hat{Q}_{i,T} - Q_T}{Q_T} - nbias\right)^2 \tag{14}$$

$$nmse = \frac{1}{N}\sum_{i=1}^{N}\left(\frac{\hat{Q}_{i,T} - Q_T}{Q_T}\right)^2 \tag{15}$$

where Q_T is the benchmark T-year return level and $\hat{Q}_{i,T}$ is the ith estimate of Q_T.

[28] Figure 8 depicts the *nbias* densities for Q_{20} with a record length of 5 years. It is overwhelming that the extremal dependence structure has a great impact on the estimation of Q_{20}. By comparing the two plots, it can be

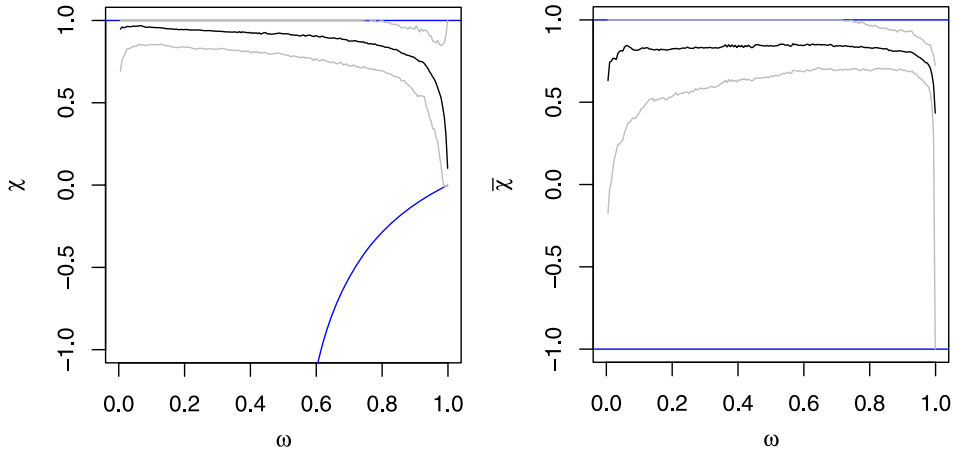

Figure 6. Plot of the χ and $\overline{\chi}$ statistics and the related 95% intervals for station A4200630. The solid blue lines are the theoretical bounds.

Table 1. The $\chi(\omega)$ Statistics for All Stations[a]

	$\omega = 0.98$		$\omega = 0.985$		$\omega = 0.99$	
Stations	$\chi(\omega)$	95% CI	$\chi(\omega)$	95% CI	$\chi(\omega)$	95% CI
A3472010	0.67	(−0.02, 1.00)	0.60	(−0.02, 1.00)	0.57	(−0.01, 1.00)
A4200630	0.53	(0.21, 0.81)	0.45	(0.07, 0.77)	0.38	(−0.01, 0.76)
A4250640	0.55	(0.27, 0.82)	0.49	(0.18, 0.76)	0.41	(0.02, 0.71)
A5431010	0.44	(−0.02, 1.00)	0.44	(−0.02, 1.00)	0.41	(−0.01, 1.00)
A5730610	0.59	(0.25, 0.94)	0.56	(0.20, 0.90)	0.50	(0.07, 0.97)
A6941010	0.62	(0.22, 0.99)	0.60	(0.16, 1.00)	0.56	(0.06, 1.00)
A6941015	0.63	(0.29, 0.95)	0.60	(0.20, 0.96)	0.58	(0.17, 0.98)
D0137010	0.39	(0.04, 0.69)	0.33	(−0.02, 0.67)	0.28	(−0.01, 0.69)
D0156510	0.59	(0.25, 0.88)	0.55	(0.20, 0.86)	0.53	(0.14, 0.92)
E1727510	0.62	(0.18, 0.91)	0.59	(0.16, 0.93)	0.47	(−0.01, 0.89)
E1766010	0.63	(0.23, 0.98)	0.59	(0.17, 0.96)	0.54	(0.09, 0.96)
E3511220	0.59	(0.10, 1.00)	0.53	(−0.02, 1.00)	0.50	(−0.01, 0.99)
E4035710	0.77	(0.02, 1.00)	0.68	(−0.02, 1.00)	0.60	(−0.01, 1.00)
E5400310	0.88	(0.30, 1.00)	0.89	(0.29, 1.00)	0.83	(0.13, 1.00)
E5505720	0.91	(0.24, 1.00)	0.87	(0.09, 1.00)	0.86	(0.02, 1.00)
E6470910	0.96	(0.40, 1.00)	0.94	(0.25, 1.00)	0.98	(0.00, 1.00)
H0400010	0.84	(0.12, 1.00)	0.83	(0.02, 1.00)	0.78	(−0.01, 1.00)
H1501010	0.82	(0.36, 1.00)	0.90	(0.39, 1.00)	0.84	(0.26, 1.00)
H2342010	0.68	(0.31, 1.00)	0.67	(0.25, 1.00)	0.60	(0.11, 1.00)
H5071010	0.75	(0.30, 1.00)	0.76	(0.22, 1.00)	0.75	(0.15, 1.00)
H5172010	0.80	(0.47, 1.00)	0.77	(0.42, 1.00)	0.73	(0.30, 1.00)
H6201010	0.69	(0.29, 1.00)	0.69	(0.14, 1.00)	0.69	(0.08, 1.00)
H7401010	0.85	(0.46, 1.00)	0.85	(0.38, 1.00)	0.81	(0.27, 1.00)
I9221010	0.67	(0.23, 1.00)	0.66	(0.19, 1.00)	0.59	(0.04, 1.00)
J0621610	0.61	(0.25, 0.92)	0.58	(0.20, 0.94)	0.51	(0.08, 0.91)
K0433010	0.59	(0.22, 0.91)	0.54	(0.15, 0.89)	0.45	(0.00, 0.85)
K0454010	0.71	(0.37, 1.00)	0.67	(0.24, 1.00)	0.65	(0.14, 1.00)
K0523010	0.62	(−0.02, 1.00)	0.58	(−0.02, 1.00)	0.53	(−0.01, 1.00)
K0550010	0.61	(0.22, 0.94)	0.57	(0.15, 0.94)	0.54	(0.07, 1.00)
K0673310	0.67	(0.24, 1.00)	0.65	(0.18, 1.00)	0.66	(0.07, 1.00)
K0910010	0.65	(−0.02, 1.00)	0.61	(−0.02, 1.00)	0.58	(−0.01, 1.00)
K1391810	0.68	(0.27, 1.00)	0.64	(0.16, 0.98)	0.60	(0.06, 0.96)
K1503010	0.69	(0.38, 0.98)	0.67	(0.30, 0.98)	0.64	(0.23, 1.00)
K2330810	0.68	(0.29, 1.00)	0.66	(0.22, 1.00)	0.62	(0.09, 1.00)
K2363010	0.65	(0.26, 0.98)	0.66	(0.16, 1.00)	0.61	(0.01, 1.00)
K2514010	0.61	(0.24, 1.00)	0.61	(0.21, 1.00)	0.58	(0.12, 1.00)
K2523010	0.53	(−0.02, 1.00)	0.53	(−0.02, 1.00)	0.51	(−0.01, 1.00)
K2654010	0.68	(0.37, 1.00)	0.68	(0.31, 1.00)	0.60	(0.10, 1.00)
K2674010	0.60	(0.25, 0.89)	0.58	(0.22, 0.94)	0.54	(0.08, 0.95)
K2871910	0.62	(0.26, 0.95)	0.57	(0.15, 0.94)	0.56	(0.10, 0.97)
K2884010	0.62	(0.25, 1.00)	0.57	(0.17, 0.97)	0.59	(0.16, 1.00)
K3222010	0.56	(0.21, 0.90)	0.53	(0.18, 0.93)	0.46	(0.11, 0.89)
K3292020	0.59	(0.27, 0.91)	0.57	(0.17, 0.91)	0.48	(0.07, 0.90)
K4470010	0.76	(0.39, 1.00)	0.77	(0.40, 1.00)	0.73	(0.27, 1.00)
K5090910	0.64	(0.27, 0.93)	0.64	(0.26, 0.96)	0.58	(0.12, 0.98)
K5183010	0.57	(0.14, 0.91)	0.56	(0.15, 0.96)	0.53	(0.06, 0.97)
K5200910	0.63	(0.24, 0.93)	0.62	(0.20, 0.95)	0.56	(0.11, 0.97)
L0140610	0.73	(0.23, 1.00)	0.66	(0.15, 1.00)	0.58	(−0.01, 1.00)
L0231510	0.59	(0.16, 0.91)	0.55	(0.11, 0.92)	0.53	(−0.01, 0.92)
L0400610	0.74	(−0.02, 1.00)	0.65	(−0.02, 1.00)	0.61	(−0.01, 1.00)

[a]Here $\omega = 0.98, 0.985, 0.99$. CI is confidence interval.

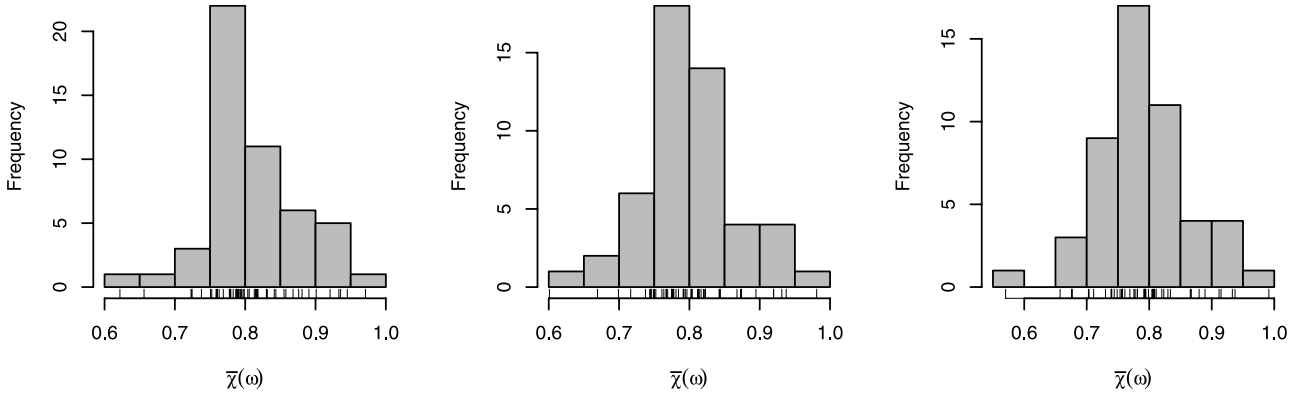

Figure 7. Histograms of the $\overline{\chi}(\omega)$ statistics for different ω values: (left) $\omega = 0.98$, (middle) $\omega = 0.985$, and (right) $\omega = 0.99$.

seen that the symmetric dependence structures give spreader densities; that is, more variable estimates. Independently of the symmetry, Figure 8 shows that the mixed dependence family is more accurate.

[29] Table 2 shows the *nbias*, *var* and *nmse* statistics for all the Markovian estimators as the record length increases for quantile Q_{50}. Table 2 confirms results derived from Figure 8. Indeed, the asymmetric dependence structures lead to less variable and biased estimates, as their *nbias* and *var* statistics are smaller. In addition, for all record length values, the Markovian models perform with the same hierarchy; that is the *mix* and *amix* models are by far the most accurate estimators, i.e., with the smallest *nmse* values. Similar results (not shown) have been obtained for other quantiles.

[30] From a hydrological point of view, these two results are not surprising. The symmetric models suppose that the variables Y_t and Y_{t+1} are exchangeable. In our context, exchangeability means that the time series is reversible, e.g., the time vector direction has no importance. When dealing with AM or POT and stationary time series, this can be a reasonable hypothesis. For example, the MLE remains the same with any permutations of the AM/POT sample. However, when modeling all exceedances, the time direction cannot be considered as reversible as flood hydrographs are clearly nonsymmetric.

[31] The Pickands dependence function $A(\omega)$ [*Pickands*, 1981] is another representation for the extremal dependence structure for any extreme value distribution. $A(\omega)$ is related to the V function in equation (3) as follows:

$$A(\omega) = \frac{V(z_1, z_2)}{z_1^{-1} + z_2^{-1}}, \qquad \omega = \frac{z_1}{z_1 + z_2} \tag{16}$$

Figure 9 represents the Pickands dependence function for all the gauging stations and the three asymmetric Markovian models. One major specificity of the mixed models is that these models cannot account for perfect dependence cases.

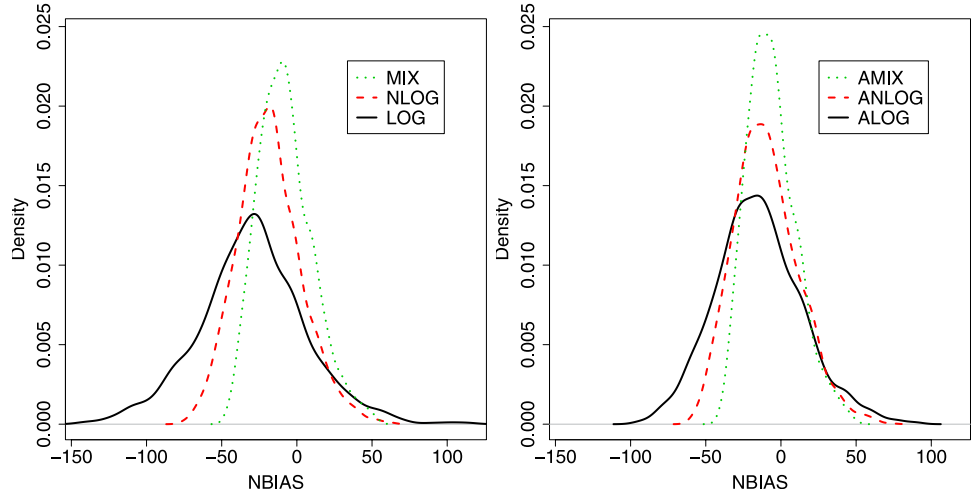

Figure 8. Densities of the normalized biases of Q_{20} estimates for (left) the symmetric Markovian models and (right) the asymmetric models. Target site record length is 5 years.

Table 2. Several Characteristics of the Markovian Estimators on Q_{50} Estimation as a Function of the Record Length[a]

	5 years			10 years			15 years			20 years		
Model	*nbias*	*var*	*nmse*	*nbias*	*var*	*nmse*	*nbias*	*var*	*nmse*	*nbias*	*var*	*nmse*
log	−0.35	0.54	0.66	−0.32	0.32	0.42	−0.30	0.23	0.32	−0.28	0.17	0.25
	(16e-3)	(22e-3)	(18e-3)	(12e-3)	(12e-3)	(14e-3)	(11e-3)	(9e-3)	(12e-3)	(9e-3)	(7e-3)	(11e-3)
nlog	−0.21	0.20	0.24	−0.20	0.11	0.15	−0.18	0.08	0.12	−0.18	0.06	0.09
	(10e-3)	(7e-3)	(11e-3)	(7e-3)	(4e-3)	(9e-3)	(6e-3)	(3e-3)	(8e-3)	(5e-3)	(2e-3)	(7e-3)
mix	−0.08	0.14	0.14	−0.07	0.08	0.08	−0.06	0.05	0.06	−0.05	0.04	0.04
	(8e-3)	(5e-3)	(8e-3)	(6e-3)	(2e-3)	(6e-3)	(5e-3)	(2e-3)	(5e-3)	(4e-3)	(1e-3)	(5e-3)
alog	−0.15	0.39	0.41	−0.13	0.22	0.24	−0.11	0.16	0.17	−0.10	0.12	0.13
	(14e-3)	(15e-3)	(14e-3)	(10e-3)	(9e-3)	(11e-3)	(9e-3)	(6e-3)	(9e-3)	(8e-3)	(4e-3)	(8e-3)
anlog	−0.10	0.20	0.21	−0.09	0.11	0.12	−0.08	0.08	0.09	−0.08	0.06	0.06
	(10e-3)	(7e-3)	(10e-3)	(7e-3)	(4e-3)	(8e-3)	(6e-3)	(2e-3)	(6e-3)	(5e-3)	(2e-3)	(6e-3)
amix	−0.06	0.11	0.12	−0.05	0.06	0.06	−0.04	0.04	0.05	−0.03	0.03	0.03
	(7e-3)	(4e-3)	(7e-3)	(6e-3)	(2e-3)	(6e-3)	(5e-3)	(1e-3)	(5e-3)	(4e-3)	(1e-3)	(4e-3)

[a]Standard errors are reported in parentheses.

In particular, the Pickands dependence functions for the mixed models satisfy $A(0.5) \geq 0.75$ while $A(0.5) \in [0.5, 1]$ for the logistic and negative logistic models. From Figure 9, it can be seen that only few stations have a dependence function that could not be modeled by the *amix* model. Therefore, the dependence range limitation of the *amix* model does not seem to be too restrictive.

[32] In this section, the effect of the extremal dependence structure was assessed. It was established that the symmetric models are hydrologically inconsistent as they could not reproduce the flood event asymmetry. In addition, for all the quantiles analyzed, the asymmetric mixed model is the most accurate for flood peak estimations. Therefore, in the remainder of this section, only the *amix* model will be compared to conventional POT estimators.

4.2. Comparison Between *amix* and Conventional POT Estimators

[33] In this section, the performance of the *amix* estimator is compared to the estimators usually used in flood frequency analysis. For this purpose, the quantile estimates derived from the maximum likelihood estimator (MLE), the unbiased and biased probability weighted moments estimators [*Hosking and Wallis*, 1987] (PWU and PWB, respectively) are considered.

[34] Figure 10 depicts the *nbias* densities for the *amix*, *MLE*, *PWU* and *PWB* estimators related to the Q_5, Q_{10} and Q_{20} estimations with a record length of 5 years. It can be seen that *amix* is the most accurate model for all quantiles. Indeed, the *amix nbias* densities are the sharpest with a mode close to 0. Focusing only on "classical" estimators (e.g., *MLE*, *PWU* and *PWB*), there is no estimator that performs systematically better than the other ones. These two results advocate the use of the *amix* model.

[35] Table 3 shows the performance of each estimator for the estimation of Q_{50} as the record length increases. It can be seen that the *amix* model performs better than the conventional estimators for the whole range of record lengths analyzed. First, *amix* has the same bias than the conventional estimators. Thus, the *amix* dependence structure seems to be suited to estimate flood quantiles. Second, because of its smaller variance, *amix* is more accurate than *MLE*, *PWU* and *PWB* estimators. This smaller variance is mainly a result of all of the exceedances (not only cluster maxima) being used in the inference procedure. Consequently, the *amix* model has a smaller *nmse*, around half of the conventional models.

[36] Figure 11 shows the evolution of the *nmse* as the return period increases for the *amix*, *MLE*, *PWU* and *PWB* models. This figure corroborates the conclusions drawn from Figure 10 and Table 3. It can be seen that the *amix* model has the smallest *nmse*, independently of the return period and the record length. In addition, the *amix* becomes increasingly more efficient as the return period increases, mostly for return periods greater than 20 years. While the conventional estimators present an erratic *nmse* behavior as the return period increases, the *amix* model is the only one that has a smooth evolution. To conclude, these results confirm that the *amix* model clearly improves flood peak quantile estimates, especially for large return periods.

5. Inference on Other Flood Characteristics

[37] As all exceedances are modeled using a first-order Markov chain, it is possible to infer other quantities than flood peaks, e.g., volume or duration. In this section, the ability of these Markovian models to reproduce flood duration is analyzed. For this purpose, the most severe flood hydrographs within each year are considered and normalized by their peak values. Consequently, from this observed normalized hydrograph set, two flood characteristics derived from a data set of hydrographs [*Robson and Reed*, 1999; *Sauquet et al.*, 2008] are considered: (1) the duration d_{mean} above 0.5 of the normalized hydrograph set mean and (2) the median d_{med} of the durations above 0.5 of each normalized hydrograph.

[38] Figure 12 illustrates the flood duration d_{mean} and d_{med} biases derived from the three asymmetric Markovian models as a function of their empirical estimates. It can be seen that no model leads to accurate flood duration estimations. In addition, the extremal dependence structure has a clear impact on these estimations. In particular, the *anlog* and *amix* models seem to underestimate flood durations, while the *alog* model leads to overestimations. Consequently, two different conclusions can be drawn. First, as large durations are poorly estimated, higher-order Markov chains

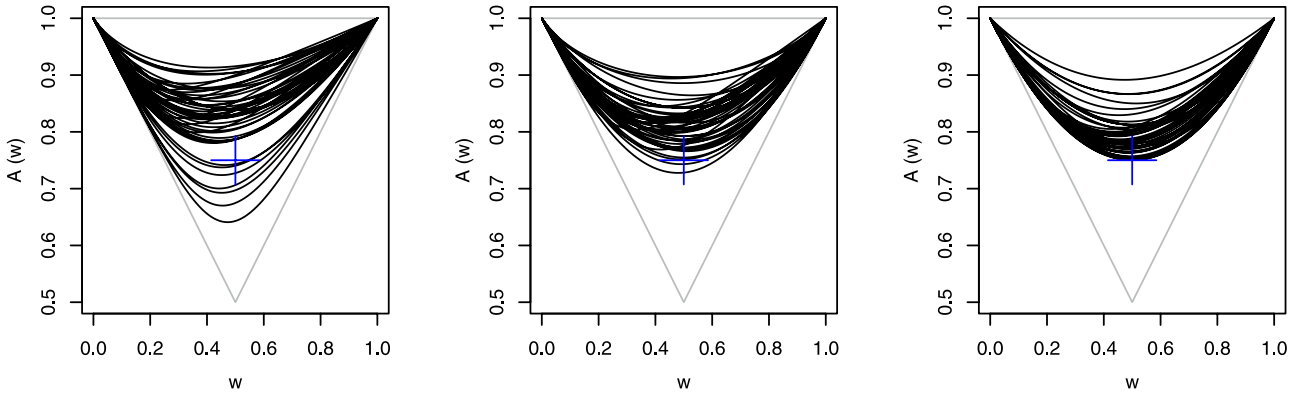

Figure 9. Representation of the Pickands dependence functions for the 50 gauging stations: (left) *alog*, (middle) *anlog*, and (right) *amix*. Pluses represent the theoretical dependence bound for the *amix* model.

may be of interest. However, this is a considerable task as higher-dimensional multivariate extreme value distributions often lead to numerical problems. Instead of considering higher-order Markov chains, another alternative may be to change daily observations for d-day observations, where d is larger than 1. Second, it is overwhelming that the extremal dependence structure affects flood duration estimations. As noticed in section 2.1, there is no finite parametrization for the extremal dependence structure V (see equation (3)). Consequently, it seems reasonable to suppose that one suited for flood hydrograph estimation may exist.

[39] Figure 13 depicts the observed normalized mean hydrographs and the ones predicted by the three asymmetric Markovian models. For the J0621610 station (left plot), the normalized hydrograph is well estimated by the three models; whereas for the L0400610 station (right plot), the normalized hydrograph is poorly predicted. This result confirms the inability of the three Markovian models to reproduce long flood events with daily data and a first-order Markov chain.

[40] Figure 14 represents the biases related to each value of the normalized mean hydrograph. The *nmse* is also reported on the right side to allow for a rational comparison of the estimators. It can be seen that the *alog* model dramatically overestimates the hydrograph rising limb while giving reasonable estimations for the recession phase. The *anlog* model slightly overestimates the rising part while strongly underestimates the recession one. The *amix* model always leads to underestimations; this is more pronounced for the falling limb. However, despite these different behaviors, these three estimators seems to have a similar performance in terms of *nmse*.

[41] Figure 15 represents the spatial distribution of the *nmse* on the normalized mean hydrograph estimation for each Markovian model. Results seem to indicate that there is a specific spatial distribution. In particular, the worst cases are located in the middle part of France. In addition, for different extremal dependence structures, the best *nmse* values correspond to different spatial locations. The *alog* model is more accurate for the extreme northern part of France; the *anlog* model is more efficient for the eastern; while the *amix* model performs best in the middle. Consequently, since at a global scale no model is accurate to estimate the normalized mean hydrograph, it is worth trying

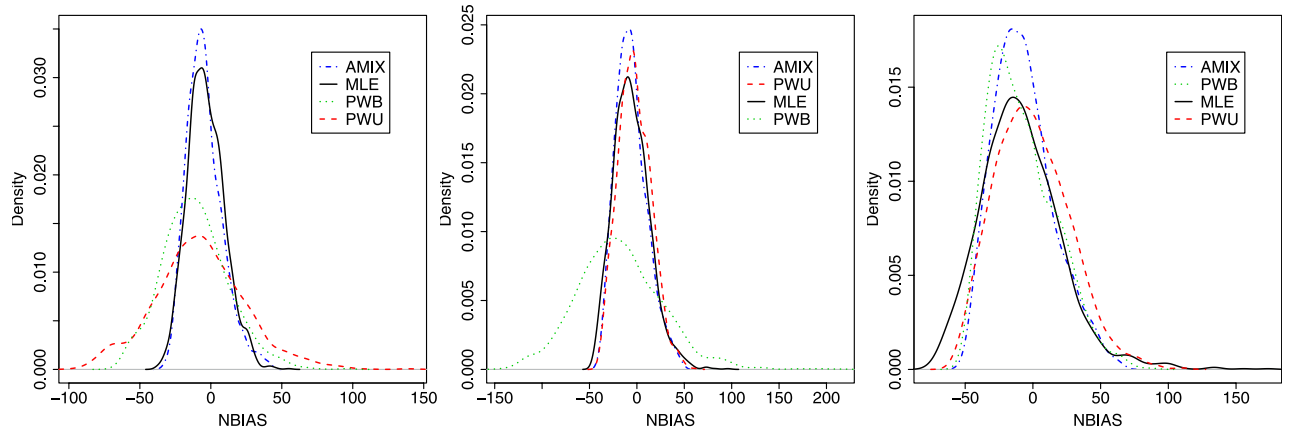

Figure 10. Densities of the normalized biases for the *amix* model and the *MLE*, *PWU*, and *PWB* estimators for quantiles (left) Q_5, (middle) Q_{10}, and (right) Q_{20}. Record length is 5 years.

Table 3. Several Characteristics of the *amix*, *MLE*, *PWU*, and *PWB* Estimators for Q_{50} Estimation as a Function of the Record Length[a]

	5 years			10 years			15 years			20 years		
Model	*nbias*	*var*	*nmse*	*nbias*	*var*	*nmse*	*nbias*	*var*	*nmse*	*nbias*	*var*	*nmse*
amix	−0.06	0.11	0.12	−0.05	0.06	0.07	−0.04	0.04	0.05	−0.04	0.03	0.03
	(8e-3)	(4e-3)	(8e-3)	(6e-3)	(2e-3)	(6e-3)	(5e-3)	(1e-3)	(5e-3)	(4e-3)	(1e-3)	(4e-3)
MLE	−0.13	0.25	0.27	−0.14	0.13	0.14	−0.13	0.08	0.10	−0.11	0.05	0.07
	(12e-3)	(15e-3)	(12e-3)	(8e-3)	(6e-3)	(9e-3)	(7e-3)	(3e-3)	(7e-3)	(5e-3)	(2e-3)	(6e-3)
PWU	0.08	0.30	0.31	−0.01	0.15	0.15	−0.03	0.10	0.10	−0.03	0.06	0.06
	(13e-3)	(13e-3)	(13e-3)	(9e-3)	(6e-3)	(9e-3)	(7e-3)	(3e-3)	(7e-3)	(6e-3)	(2e-3)	(6e-3)
PWB	−0.07	0.20	0.21	−0.10	0.11	0.12	−0.11	0.08	0.09	−0.10	0.05	0.06
	(10e-3)	(8e-3)	(11e-3)	(7e-3)	(4e-3)	(8e-3)	(6e-3)	(2e-3)	(7e-3)	(5e-3)	(1e-3)	(6e-3)

[a]Standard errors are reported in parentheses.

to identify which catchment types are related to the best estimations.

[42] For the data set of the present case study, this is a considerable task. No standard statistical technique leads to reasonable results. In particular, the principal component analysis, hierarchical classification, sliced inverse regression lead to no conclusion concerning which catchment types are more suitable for our models. Only a regression approach gives some first guidelines. For this purpose, a regression between the *nbias* on the d_{mean} estimation for each asymmetric model and some geomorphologic and hydrologic indices are performed. The effect of the drainage area, an index of catchment slope derived from the hypsometric curve [*Roche*, 1963], the base flow index (BFI) [*Tallaksen and Van Lanen*, 2004, section 5.3.3] and an index characterizing the rainfall persistence [*Vaskova and Francès*, 1998] are considered:

$$nbias(d_{mean}; anlog) = 0.89 - 2.19BFI, \quad R^2 = 0.40 \qquad (17)$$

$$nbias(d_{mean}; amix) = 0.49 - 1.74BFI, \quad R^2 = 0.43 \qquad (18)$$

[43] From equations (17) and (18), it can be seen that the *BFI* variable explains around 40% of the variance. Despite

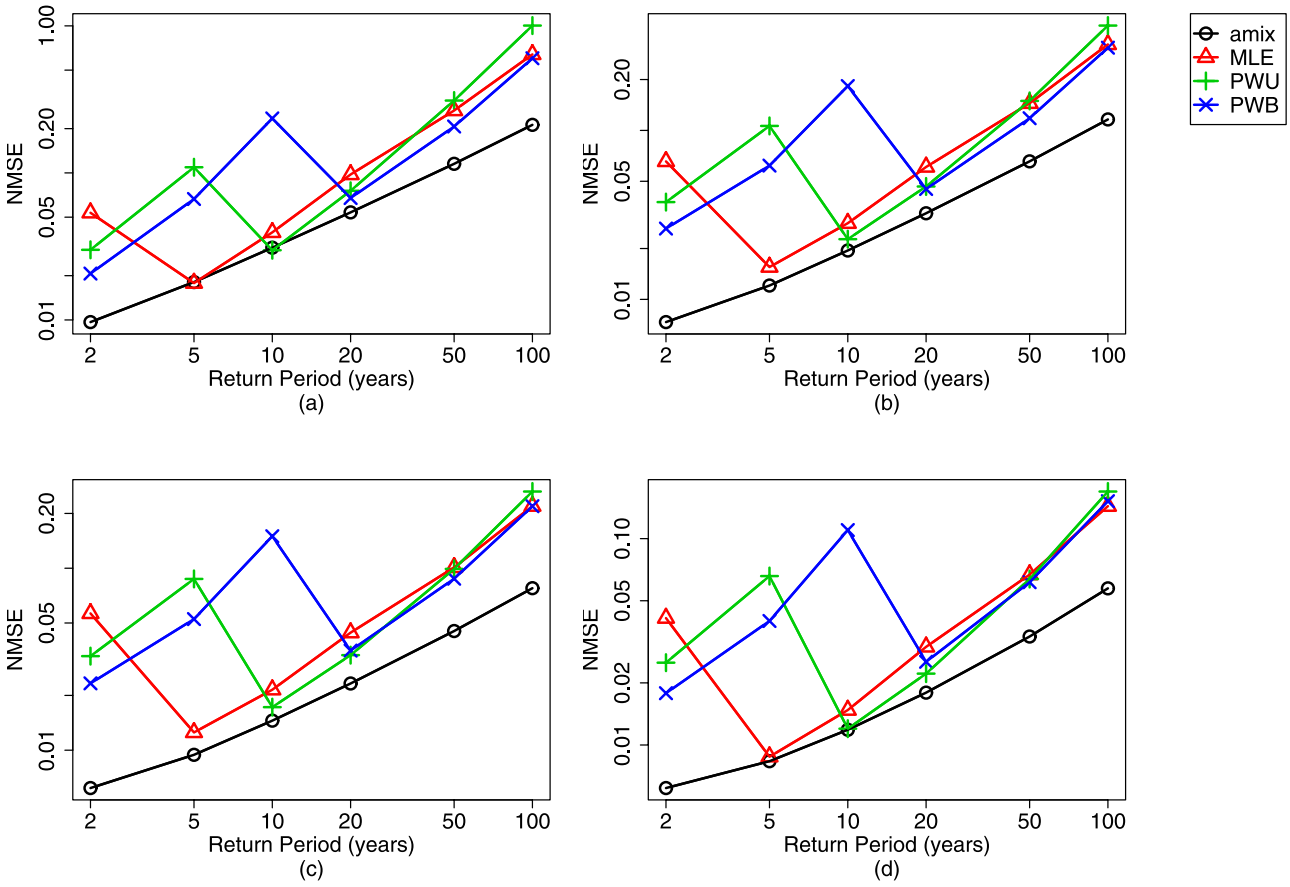

Figure 11. Evolution of the *nmse* as a function of the return period for the *amix*, *MLE*, *PWU*, and *PWB* estimators. Record length: (a) 5 years, (b) 10 years, (c) 15 years, and (d) 20 years.

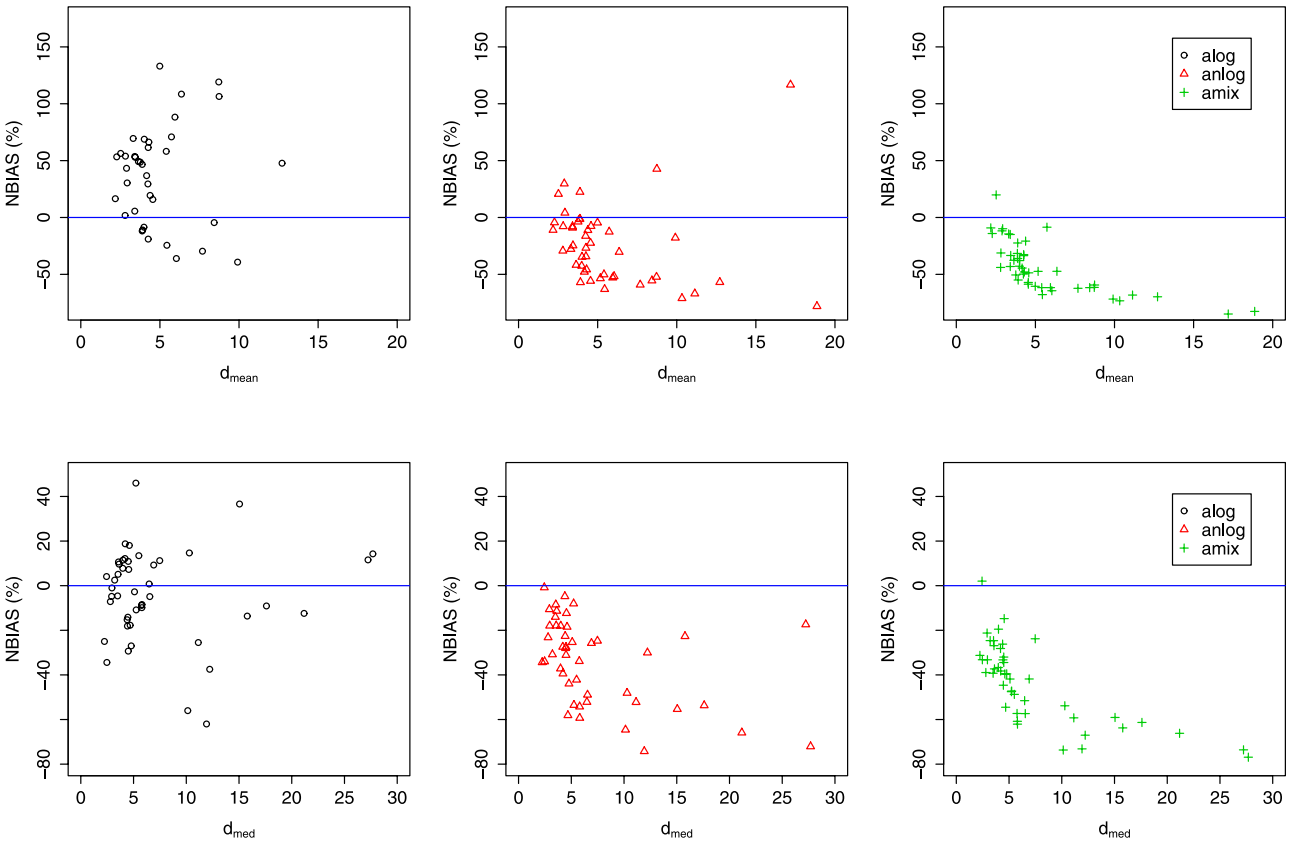

Figure 12. The d_{mean} and d_{med} normalized biases as a function of the theoretical values for the three asymmetric Markovian models.

the fact that a large variance proportion is not taken into account, the *BFI* is clearly related to the d_{mean} estimation performance. These equations indicate that the *anlog* (*amix*) model is more accurate to reproduce the d_{mean} variable for gauging stations with a *BFI* around 0.4 (0.28). These *BFI* values correspond to catchments with moderate up to flash flow regimes respectively. These results corroborate the ones derived from Figure 14: the first-order Markovian models with a 1-day lag conditioning are not appropriate for long flood duration estimations. Consequently, while no physiographic characteristic is related to the *alog* performance, it is suggested, for such 1-day lag conditioning, to use the *anlog* and *amix* models for quick basins.

6. Conclusions and Perspectives

[44] Despite the fact that univariate EVT is widely applied in environmental sciences, its multivariate extension is rarely considered. This work tries to promote the use of the MEVT in hydrology. In this work, the bivariate case was

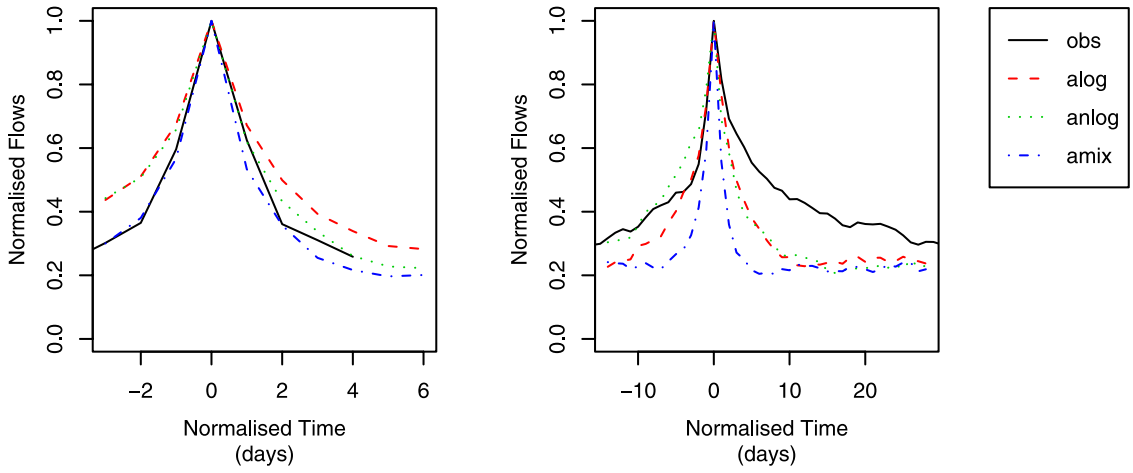

Figure 13. Observed and simulated normalized mean hydrographs for the (left) J0621610 and (right) L0400610 stations.

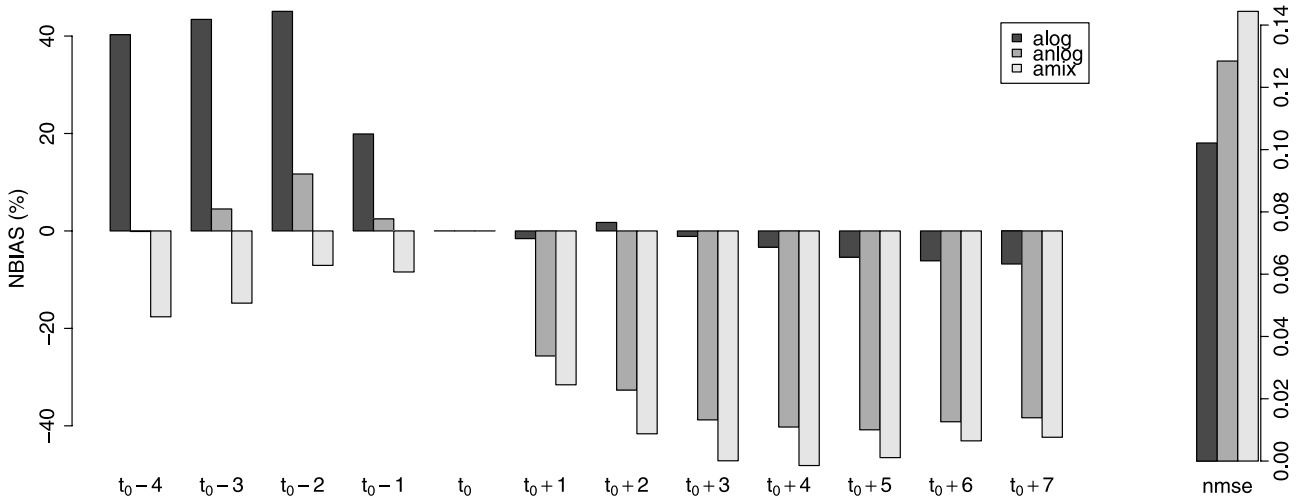

Figure 14. Evolution of the biases for the normalized mean hydrograph estimations as a function of the distance from the flood peak time.

considered as the dependence between two successive observations was modeled using a first-order Markov chain. This approach has two main advantages for practitioners as (1) the amount of data to be inferred increases considerably and (2) other features can be estimated: flood duration, volume.

[45] In this study, a comparison between six different extremal dependence structures (including both symmetric and asymmetric forms) was carried out. Results show that an asymmetric dependence structure is more relevant. From a hydrological point of view, this asymmetry is rational as flood hydrographs are asymmetric. In particular, for our data, the asymmetric mixed model gives the most accurate flood peak estimations and clearly improves flood peak estimations in comparison to conventional estimators, independently of the return period considered.

[46] The ability of these Markovian models to estimate flood duration was also studied. It was shown that, at first sight, no dependence structure is able to reproduce the flood hydrograph accurately. However, it seems that the *anlog* and *amix* models may be more appropriate when dealing with moderate up to flash flow regimes. These results depend strongly on the conditioning term (i.e., $\Pr[Y_t \leq y_t | Y_{t-\delta} = y_{t-\delta}]$) of the first-order Markov chain and on the autocorrelation within the time series. In our application, $\delta = 1$ and a daily time step was considered.

[47] More general conclusions can be drawn. The weakness of the proposed models to derive consistent flood hydrographs may not be related to the daily time step but to the inadequacy between the conditioning term and the flood dynamics. To ensure better results, higher-order Markov chains may be of interest [*Fawcett and Walshaw*, 2006]. However, as numerical problems may arise, another alternative may be to still consider a first-order chain but to change the "conditioning lag value" δ. In particular, for some basins, it may be more relevant to condition the Markov chain with a larger but more appropriate lag value.

[48] Another option to improve the proposed models for flood hydrograph estimation is to use a more suitable dependence function *V*. As there is no finite parametrization

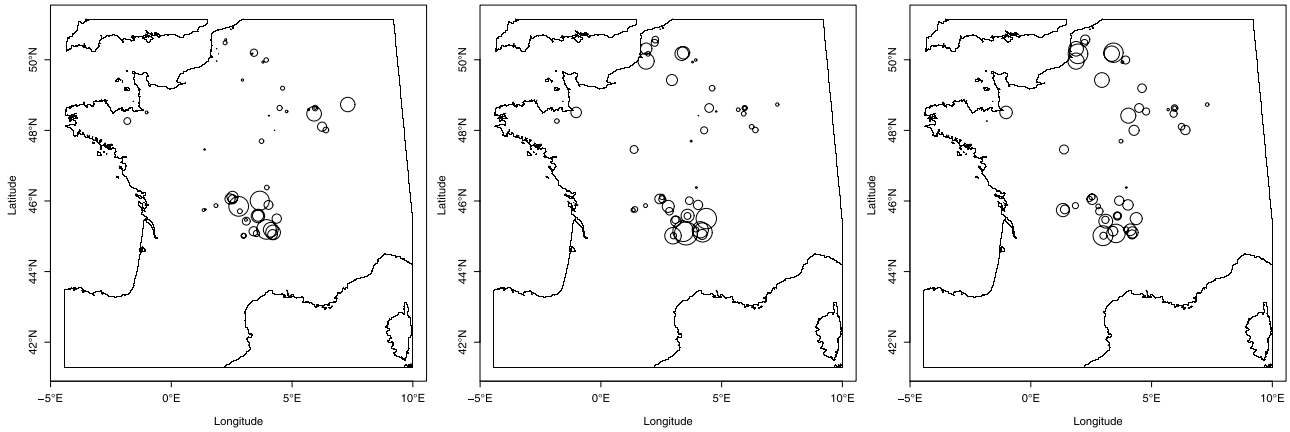

Figure 15. The *nmse* spatial distribution according to the three Markovian models: (left) *alog*, (middle) *anlog*, and (right) *amix*. The radius is proportional to the *nmse* value.

Table A1. Partial and Mixed Partial Derivatives, Definition Domain, and Total Independent and Perfect Dependent Cases for Each Extremal Symmetric Dependence Function V

	Symmetric Models		
Model	*log*	*nlog*	*mix*
$V(x, y)$	$(x^{-1/\alpha} + y^{-1/\alpha})^{\alpha}$	$\frac{1}{x} + \frac{1}{y} - (x^{\alpha} + y^{\alpha})^{-1/\alpha}$	$\frac{1}{x} + \frac{1}{y} - \frac{\alpha}{x+y}$
$V_1(x, y)$	$-x^{-\frac{1}{\alpha}-1} V(x, y)^{\frac{\alpha-1}{\alpha}}$	$-\frac{1}{x^2} + x^{\alpha-1}(x^{\alpha} + y^{\alpha})^{-\frac{1}{\alpha}-1}$	$-\frac{1}{x^2} + \frac{\alpha}{(x+y)^2}$
$V_2(x, y)$	$-y^{-\frac{1}{\alpha}-1} V(x, y)^{\frac{\alpha-1}{\alpha}}$	$-\frac{1}{y^2} + y^{\alpha-1}(x^{\alpha} + y^{\alpha})^{-\frac{1}{\alpha}-1}$	$-\frac{1}{y^2} + \frac{\alpha}{(x+y)^2}$
$V_{12}(x, y)$	$-(xy)^{-\frac{1}{\alpha}-1} \frac{1-\alpha}{\alpha} V(x, y)^{\frac{\alpha-2}{\alpha}}$	$-(\alpha + 1)(xy)^{\alpha-1}(x^{\alpha} + y^{\alpha})^{-\frac{1}{\alpha}-2}$	$-\frac{2\alpha}{(x+y)^3}$
$A(w)$	$[(1 - w)^{\frac{1}{\alpha}} + w^{\frac{1}{\alpha}}]^{\alpha}$	$1 - [(1 - w)^{-\alpha} + w^{-\alpha}]^{-\frac{1}{\alpha}}$	$1 - w(1 - w)\alpha$
Independence	$\alpha = 1$	$\alpha \to 0$	$\alpha = 0$
Total dependence	$\alpha \to 0$	$\alpha \to +\infty$	Never reached
Constraint	$0 < \alpha \leq 1$	$\alpha > 0$	$0 \leq \alpha \leq 1$

for the extremal dependence structure, it seems reasonable that one more appropriate for flood hydrographs may exist. In this work, results show that the *anlog* model is more able to reproduce the hydrograph rising part, while the *alog* is better for the recession phase. One alternative is to define

$$V(z_1, z_2) = \alpha V_1(z_1, z_2) + \beta V_2(z_1, z_2)$$

where V_1 (V_2) is the extremal dependence function for the *alog* (*anlog*) model and α and β are real constants such that $\alpha + \beta = 1$. By definition, V is a new extremal dependence function. In particular, V may combine the accuracy of the *alog* and *anlog* models for both the rising and recession part of the flood hydrograph. Another alternative may be to look at the nonparametric Pickands dependence function estimators [*Capéraà et al.*, 1997] but this will require techniques to simulate Markov chains from these nonparametric estimations.

[49] Finally, the models proposed in this article were asymptotically dependent. Recently, *Heffernan and Tawn* [2004] proposed a semiparametric approach allowing for asymptotic independence and which can be applied to problems of any dimension. This semiparametric approach might be appropriate when asymptotic dependence seems too restrictive and/or k-order Markov chain models, $k > 1$, should be considered.

[50] All statistical analysis were performed within the *R Development Core Team* [2007] framework. In particular, the POT package [*Ribatet*, 2007] integrates the tools that were developed to carry out the modeling effort presented in this paper. This package is available, free of charge, at the Web site http://www.r-project.org, section CRAN, Packages or at its own Web page http://pot.r-forge.r-project.org/.

Appendix A: Parametrization for the Extremal Dependence

[51] This appendix presents some useful results for the six extremal dependence models that have been considered in this work. As first-order Markov chains were used, only the bivariate results are described. The expressions of the partial and mixed partial derivatives, the Pickands dependence function and the limiting dependence cases are reported in Tables A1 and A2.

Table A2. Partial and Mixed Partial Derivatives, Definition Domain, and Total Independent and Perfect Dependent Cases for Each Extremal Asymmetric Dependence Function V

	Asymmetric Models		
Model	*alog*	*anlog*	*amix*
$V(x, y)$	$\frac{1-\theta_1}{x} + \frac{1-\theta_2}{y} + \left[\left(\frac{x}{\theta_1}\right)^{-1/\alpha} + \left(\frac{y}{\theta_2}\right)^{-1/\alpha}\right]^{\alpha}$	$\frac{1}{x} + \frac{1}{y} - \left[\left(\frac{x}{\theta_1}\right)^{\alpha} + \left(\frac{y}{\theta_2}\right)^{\alpha}\right]^{-1/\alpha}$	$\frac{1}{x} + \frac{1}{y} - \frac{(2\alpha+\theta)x+(\alpha+\theta)y}{(x+y)^2}$
$V_1(x, y)$	$-\frac{1-\theta_1}{x^2} - \theta_1^{\frac{1}{\alpha}} x^{-\frac{1}{\alpha}-1}\left[\left(\frac{x}{\theta_1}\right)^{-1/\alpha} + \left(\frac{y}{\theta_2}\right)^{-1/\alpha}\right]^{\alpha-1}$	$-\frac{1}{x^2} + \theta_1^{-\alpha} x^{\alpha-1}\left[\left(\frac{x}{\theta_1}\right)^{\alpha} + \left(\frac{y}{\theta_2}\right)^{\alpha}\right]^{-1/\alpha-1}$	$-\frac{1}{x^2} - \frac{2\alpha+\theta}{(x+y)^2} + 2\frac{(2\alpha+\theta)x+(\alpha+\theta)y}{(x+y)^3}$
$V_2(x, y)$	$-\frac{1-\theta_2}{y^2} - \theta_2^{\frac{1}{\alpha}} y^{-\frac{1}{\alpha}-1}\left[\left(\frac{x}{\theta_1}\right)^{-1/\alpha} + \left(\frac{y}{\theta_2}\right)^{-1/\alpha}\right]^{\alpha-1}$	$-\frac{1}{y^2} + \theta_2^{-\alpha} y^{\alpha-1}\left[\left(\frac{x}{\theta_1}\right)^{\alpha} + \left(\frac{y}{\theta_2}\right)^{\alpha}\right]^{-1/\alpha-1}$	$-\frac{1}{y^2} - \frac{\alpha+\theta}{(x+y)^2} + 2\frac{(2\alpha+\theta)x+(\alpha+\theta)y}{(x+y)^3}$
$V_{12}(x, y)$	$\frac{\alpha-1}{\alpha}(\theta_1\theta_2)^{\frac{1}{\alpha}}(xy)^{-\frac{1}{\alpha}-1}\left[\left(\frac{x}{\theta_1}\right)^{-1/\alpha} + \left(\frac{y}{\theta_2}\right)^{-1/\alpha}\right]^{\alpha-2}$	$-(\alpha + 1)(\theta_1\theta_2)^{-\alpha}(xy)^{\alpha-1}\left[\left(\frac{x}{\theta_1}\right)^{\alpha} + \left(\frac{y}{\theta_2}\right)^{\alpha}\right]^{-1/\alpha-2}$	$\frac{6\alpha+4\theta}{(x+y)^3} - 6\frac{(2\alpha+\theta)x+(\alpha+\theta)y}{(x+y)^4}$
$A(w)$	$(1 - \theta_1)(1 - w) + (1 - \theta_2)w + [(1 - w)^{\frac{1}{\alpha}}\theta_1^{\frac{1}{\alpha}} + w^{\frac{1}{\alpha}}\theta_2^{\frac{1}{\alpha}}]^{\alpha}$	$1 - \left[\left(\frac{1-w}{\theta_1}\right)^{-\alpha} + \left(\frac{w}{\theta_2}\right)^{-\alpha}\right]^{-\frac{1}{\alpha}}$	$\theta w^3 + \alpha w^2 - (\alpha + \theta)w + 1$
Independence	$\alpha = 1$ or $\theta_1 = 0$ or $\theta_2 = 0$	$\alpha \to 1$ or $\theta_1 \to 0$ or $\theta_2 \to = 0$	$\alpha = \theta = 0$
Total dependence	$\alpha \to 0$	$\alpha \to +\infty$	Never reached
Constraint	$0 < \alpha \leq 1$, $0 \leq \theta_1, \theta_2 \leq 1$	$\alpha > 0$, $0 < \theta_1, \theta_2 \leq 1$	$\alpha \geq 0$, $\alpha + 2\theta \leq 1$, $\alpha + 3\theta \geq 0$

[52] **Acknowledgments.** The authors wish to thank the French HYDRO (http://www.hydro.eaufrance.fr/) database for providing the data. The authors wish also to thank the associate editor and three anonymous reviewers whose comments helped improve considerably the quality of the manuscript.

References

Ashkar, F., and J. Rousselle (1987), Partial duration series modeling under the assumption of a Poissonian flood count, *J. Hydrol.*, *90*, 135–144.

Ashkar, F., N. El Jabi, and M. Issa (1998), A bivariate analysis of the volume and duration of low-flow events, *Stochastic Hydrol. Hydraul.*, *12*, 97–116.

Bortot, P., and S. Coles (2000), The multivariate Gaussian tail model: An application to oceanographic data, *J. R. Stat. Soc., Ser. C*, *49*(1), 31–49.

Bortot, P., and J. A. Tawn (1998), Models for the extremes of Markov chains, *Biometrika*, *85*(4), 851–867.

Capéraà, P., A.-L. Fougères, and C. Genest (1997), A nonparametric estimation procedure for bivariate extreme value copulas, *Biometrika*, *84*(3), 567–577.

Chebana, F., and T. B. M. J. Ouarda (2007), Multivariate L-moment homogeneity test, *Water Resour. Res.*, *43*, W08406, doi:10.1029/2006WR005639.

Chebana, F., and T. B. M. J. Ouarda (2008), Depth and homogeneity in regional flood frequency analysis, *Water Resour. Res.*, *44*, W11422, doi:10.1029/2007WR006771.

Coles, S. (2001), *An Introduction to Statistical Modeling of Extreme Values*, Springer, London.

Coles, S., and J. A. Tawn (1991), Modelling extreme multivariate events, *J. R. Stat. Soc., Ser. B*, *53*(2), 377–392.

Coles, S., J. A. Tawn, and R. L. Smith (1994), A seasonal Markov model for extremely low temperature, *Environmetrics*, *5*, 221–239.

Coles, S., J. Heffernan, and J. A. Tawn (1999), Dependence measures for extreme value analyses, *Extremes*, *2*(4), 339–365.

Cunderlik, J. M., and T. B. M. J. Ouarda (2006), Regional flood-duration-frequency modeling in the changing environment, *J. Hydrol.*, *318*, 276–291.

Falk, M., and R. Michel (2006), Testing for tail independence in extreme value models, *Ann. Inst. Stat. Math.*, *58*(2), 261–290.

Fawcett, L. (2005), Statistical methodology for the estimation of environmental extremes, Ph.D. thesis, Univ. of Newcastle upon Tyne, Newcastle upon Tyne, U. K.

Fawcett, L., and D. Walshaw (2006), Markov chain models for extreme wind speeds, *Environmetrics*, *17*, 795–809.

Ferro, C. A. T., and J. Segers (2003), Inference for clusters of extreme values., *J. R. Stat. Soc., Ser. B*, *65*(2), 545–556.

Galambos, J. (1975), Order statistics of samples from multivariate distributions, *J. Am. Stat. Assoc.*, *9*, 674–680.

Gumbel, E. J. (1960), Bivariate exponential distributions, *J. Am. Stat. Assoc.*, *55*, 698–707.

Heffernan, J. E., and J. A. Tawn (2004), A conditional approach for multivariate extreme values, *J. R. Stat. Soc., Ser. B*, *66*(3), 497–530.

Hosking, J. R. M., and J. R. Wallis (1987), Parameter and quantile estimation for the generalized Pareto distribution, *Technometrics*, *29*(3), 339–349.

Joe, H. (1990), Families of min-stable multivariate exponential and multivariate extreme value distributions, *Stat. Probab. Lett.*, *9*, 75–82.

Kjeldsen, T. R., and D. A. Jones (2006), Prediction uncertainty in a median-based index flood method using L moments, *Water Resour. Res.*, *42*, W07414, doi:10.1029/2005WR004069.

Kjeldsen, T. R., and D. Jones (2007), Estimation of an index flood using data transfer in the UK, *Hydrol. Sci. J.*, *52*(1), 86–98.

Leadbetter, M. R. (1983), Extremes and local dependence in stationary sequences, *Probab. Theory Related Fields*, *65*(2), 291–306.

Ledford, A. W., and J. A. Tawn (1996), Statistics for near independence in multivariate extreme values, *Biometrika*, *83*, 169–187.

Ledford, A. W., and J. A. Tawn (2003), Diagnostics for dependence within time series extremes, *J. R. Stat. Soc., Ser. B*, *65*(2), 521–543.

Lindgren, G., and H. Rootzen (1987), Extreme values: Theory and technical applications, *Scand. J. Stat.*, *14*(4), 241–279.

Madsen, H., and D. Rosbjerg (1997), Generalized least squares and empirical Bayes estimation in regional partial duration series index-flood modeling, *Water Resour. Res.*, *33*(4), 771–781.

Ouarda, T. B. M. J., C. Charron, and A. St-Hilaire (2008), Statistical models and the estimation of low flows, *Can. Water Resour. J.*, *33*(2), 195–206.

Pickands, J. (1981), Multivariate extreme value distributions, paper presented at 43rd Session, Int. Stat. Inst., Buenos Aires.

R Development Core Team (2007), *R: A Language and Environment for Statistical Computing*, R Found. for Stat. Comput., Vienna.

Reis, D. S., Jr., and J. R. Stedinger (2005), Bayesian MCMC flood frequency analysis with historical information, *J. Hydrol.*, *313*, 97–116.

Renard, B., et al. (2008), Regional methods for trend detection: Assessing field significance and regional consistency, *Water Resour. Res.*, *44*, W08419, doi:10.1029/2007WR006268.

Resnick, S. I. (1987), *Extreme Values, Regular Variation and Point Processes*, Springer, New York.

Ribatet, M. (2007), POT: Modelling peaks over a threshold, *R News*, *7*(1), 34–36.

Ribatet, M., E. Sauquet, J.-M. Grésillon, and T. B. M. J. Ouarda (2007a), A regional Bayesian POT model for flood frequency analysis, *Stochastic Environ. Res. Risk Assess.*, *21*(4), 327–339.

Ribatet, M., E. Sauquet, J. M. Grsillon, and T. B. M. J. Ouarda (2007b), Usefulness of the reversible jump Markov chain Monte Carlo model in regional flood frequency analysis, *Water Resour. Res.*, *43*, W08403, doi:10.1029/2006WR005525.

Robson, A. J., and D. W. Reed (1999), *Flood Estimation Handbook*, vol. 3, Inst. of Hydrol., Wallingford, U. K.

Roche, M. (1963), *Hydrologie de Surface*, Gauthier-Villars, Paris.

Salvadori, G., and C. De Michele (2004), Analytical calculation of storm volume statistics involving Pareto-like intensity-duration marginals, *Geophys. Res. Lett.*, *31*, L04502, doi:10.1029/2003GL018767.

Sauquet, E., M.-H. Ramos, L. Chapel, and P. Bernardara (2008), Stream flow scaling properties: Investigating characteristic scales from different statistical approaches, *Hydrol. Processes*, *22*(17), 3462–3475, doi:10.1002/hyp.6952.

Smith, R. L., J. A. Tawn, and S. G. Coles (1997), Markov chain models for threshold exceedances, *Biometrika*, *84*(2), 249–268.

Tallaksen, L., and H. Van Lanen (Eds.) (2004), *Hydrological Drought: Processes and Estimation Methods for Streamflow and Groundwater*, *Dev. Water Sci.*, vol. 48, Elsevier, Amsterdam.

Tawn, J. A. (1988), Bivariate extreme value theory: Models and estimation, *Biometrika*, *75*(3), 397–415.

Vaskova, I., and F. Francès (1998), Rainfall analysis and regionalization computing intensity-duration-frequency curves, Floodaware final report. Programme Climate and Environment 1994–1998. Area 2.3.1: Hydrological and hydrogeological risks, *Contract ENV4-CT96-0293*, Cemagref, Lyon, France.

Werritty, A., J. L. Paine, N. Macdonald, J. S. Rowan, and L. J. McEwen (2006), Use of multi-proxy flood records to improve estimates of flood risk: Lower River Tay, Scotland, *Catena*, *66*(1–2), 107–119.

Yue, S., T. B. M. J. Ouarda, and B. Bobee (2001), A review of bivariate gamma distributions, *J. Hydrol.*, *246*, 1–18.

Zhang, L., and V. P. Singh (2006), Bivariate flood frequency analysis using the copula method, *J. Hydrol Eng.*, *11*, 150–164.

J.-M. Gresillon and E. Sauquet, Cemagref Lyon, Unite de Recherche Hydrologie-Hydraulique, 3 bis quai Chauveau, CP220, F-69336 Lyon CEDEX 09, France. (jean-michel.gresillon@cemagref.fr; eric.sauquet@cemagref.fr)

T. B. M. J. Ouarda, INRS-ETE, University of Quebec, 490, de la Couronne Quebec, QC G1K 9A9, Canada. (taha_ouarda@ete.inrs.ca)

M. Ribatet, Institute of Mathematics, Station 8, Ecole Polytechnique Federale de Lausanne, CH-1015 Lausanne, Switzerland. (mathieu.ribatet@epfl.ch)